Polymer Vol. 39 No. 18, pp. 4235–4241, 1998

0032-3861/98/$19.00+0.00

PII: S0032-3861(98)00111-6

Application of a zone-drawing and zone-annealing method to poly(ethylene-2,6-naphthalate) fibres

Akihiro Suzuki*, Takayoshi Kuwabara and Toshio Kunugi
Department of Applied Chemistry and Biotechnology, Faculty of Engineering, Yamanashi University, 4-3-11 Takeda, Kofu 400-8511, Japan
(Received 25 November 1997; revised 5 January 1998; accepted 29 January 1998)

A zone-drawing and zone-annealing method was applied to poly(ethylene-2,6-naphthalate) fibres in order to improve their mechanical properties. The zone-drawing was carried out at a drawing temperature of 130°C under an applied tension of 13 MPa, and the zone-annealing was carried out at an annealing temperature of 200°C under 212 MPa. The zone-annealed fibre had a birefringence of 0.473 and degree of crystallinity of 40%. Wide-angle X-ray diffraction photographs of the zone-drawn and zone-annealed fibres showed three reflections (010, 100, and $\bar{1}10$) attributed to an α-form crystal, but no (020) reflection attributed to a β-form was observed in the equator. The tensile modulus and tensile strength increase with processing, and the zone-annealed fibre has a modulus of 29 GPa and a tensile strength of 1.1 GPa.

(Keywords: poly(ethylene-2,6-naphthalate) fibre; zone-drawing and zone-annealing; mechanical properties)

INTRODUCTION

Poly(ethylene-2,6-naphthalate) (PEN) is a high-temperature semicrystalline thermoplastic polymer that combines the properties of excellent chemical resistance, flame resistance, and mechanical strength. However, so far the PEN has hardly been used in industry because of the high cost of the production of intermediates. The applications of PEN films to a high-performance magnetic tape and a heat-resistant insulating tape have been considered recently.

There are two known crystal morphologies[1]: an α-form and a β-form. The α-form[2] is a triclinic unit cell with the unit-cell parameters $a = 0.651$ nm, $b = 0.575$ nm, $c = 1.32$ nm, $\alpha = 81.33°$, $\beta = 144°$, and $\gamma = 100°$. One chain passes though each unit cell. The β-form[1] is also a triclinic unit cell with the unit-cell parameters $a = 0.926$ nm, $b = 1.559$ nm, $c = 1.273$ nm, $\alpha = 121.6°$, $\beta = 95.57°$, and $\gamma = 122.52°$. Four chains pass though each cell. The chains are not completely extended; every naphthalene ring is twisted by 180°.

Numerous studies[3–10] have been undertaken to investigate the crystalline structure, morphology, thermal stability, and crystallization kinetics of PEN. Few investigations[11,12] have been carried out on the mechanical properties of PEN fibres. Mechanical properties of PEN are higher than those of PET because PEN contains a naphthalene ring instead of the benzene ring in PET. Nakamae *et al.*[13,14] reported that the elastic modulus (E_1) of the crystalline regions of PEN in the direction parallel to the chain axis was 145 GPa at room temperature. The E_1 value of PEN is higher than that of PET (110 GPa at room temperature[15]).

Many studies[16–21] have been carried out in the development of high-modulus and high-strength fibres. A zone-drawing and zone-annealing (ZD and ZA) method is one of the techniques leading to high-modulus and high-strength fibres. The ZD and ZA method has already been applied to many polymers, such as poly(ethylene terephthalate) (PET)[22], it-polypropylene [23,24], nylon 6[25,26], nylon 66[27], nylon 46[28], poly(vinyl alcohol)[29], poly(ether ether ketone)[30], and poly(*p*-phenylene sulfide)[31] fibres to improve their mechanical properties. This treatment was capable of leading to the high-modulus and high-strength fibres.

It is the purpose of the present paper to determine optimum conditions for the ZD and the ZA treatments and to discuss the changes in the microstructure and the mechanical properties with the treatment. Their changes with processing were investigated using a tensile testing machine, a dynamic viscoelastometer, differential scanning calorimetry, thermal mechanical analysis, wide-angle X-ray diffraction, birefringence, and density measurements.

EXPERIMENTAL

Material

The original material used in the present study was the as-spun PEN fibre supplied by Teijin Ltd. The original fibre had a diameter of about 0.379 mm, degree of crystallinity of 4%, birefringence of 3×10^{-3}, and an intrinsic viscosity of 0.63 dl g^{-1}. The original fibre was found to be amorphous and isotropic from a wide-angle X-ray diffraction photograph as shown in *Figure 1*.

Apparatus for zone-drawing and zone-annealing

The ZD and ZA treatments were carried out by using an apparatus similar to that described in detail elsewhere[25].

Measurement

The draw ratio was determined in the usual way by measuring the displacement of ink marks placed 10 mm apart on the fibre prior to drawing. The density (ρ) of the fibre was measured at 23°C by flotation using a carbon

* To whom correspondence should be addressed

tetrachloride and toluene mixture. The degree of crystallinity, expressed as a weight fraction (X_w), was obtained using the relation:

$$X_w = \{\rho_c(\rho - \rho_a)\}/\{\rho(\rho_c - \rho_a)\} \times 100 \quad (1)$$

where ρ_c and ρ_a are densities of crystalline and amorphous phases, respectively. In this measurement, values of 1.407 and 1.325 g cm^{-3} were assumed for ρ_c[32] and for ρ_a[33], respectively. The density of amorphous polymer was assumed to be constant, independently of treatments.

Orientation factors of crystallites (f_c) were evaluated by using the Wilchinsky method[34] from wide-angle X-ray diffraction patterns.

Wide-angle X-ray diffraction (WAXD) patterns of the fibres were taken using a WAXD camera. The camera was attached to a Rigaku X-ray generator which was operated at 40 kV and 25 mA. The radiation used was Ni-filtered Cu Kα (wavelength 1.542 Å). The sample-to-film distance was 40 mm. The fibre was exposed for 2.5 h to the X-ray beam from a pinhole collimator with a diameter of 0.4 mm.

Differential scanning calorimetry (d.s.c.) measurements were carried out using a Rigaku DSC 8230C calorimeter. The d.s.c. scans were performed within the temperature range from 25 to 300°C, using a heating rate of 10°C min^{-1}. All measurements were carried out under a nitrogen purge. The d.s.c. instrument was calibrated with indium.

Thermal shrinkage was measured with a Rigaku SS-TMA at a heating rate of 5°C min^{-1}. The samples with a 15 mm gauge length between two jaws were held at a tension of 5 g cm^{-2}, which was the minimum tension to stretch a fibre tightly.

A Tensilon tensile testing machine was used to determine tensile modulus, tensile strength, and elongation at break. A gauge length of 5 cm and elongation rate of 10 mm min^{-1} were used. The measurements were carried out at 23°C, and relative humidity of 65%. The dynamic viscoelastic properties were measured at 110 Hz with a dynamic viscoelastometer Vibron DDV-II (Orientec Co. Ltd.). Measurements were carried out over a temperature range of 30°C to about 250°C at intervals of 5°C, and the average heating rate was 2°C min^{-1}. A single fibre was held at a 20 mm gauge length between two jaws.

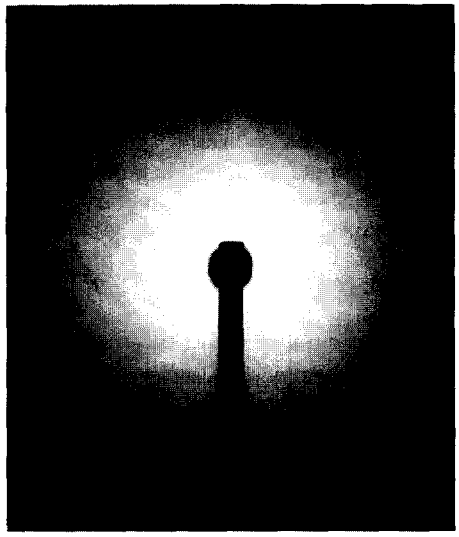

Figure 1 Wide-angle X-ray diffraction photograph of the original PEN fibre

RESULTS AND DISCUSSION

Determination of optimum condition for the zone-drawing

The mechanical properties of semicrystalline polymers such as nylon 6, nylon 66, and poly(ethylene terephthalate) depend chiefly on the amorphous regions rather than crystalline regions because they have only a degree of crystallinity of the order of 50%–60%. Therefore, the improvements of their mechanical properties would be achieved by increasing the number of the tie chains in the amorphous regions and making uniform those lengths so that applied stress may be loaded equally on the fibre[35–37]. Fortunately, since the as-spun PEN fibre as well as PET is to be amorphous, one could conjecture that molecular chains are easily aligned parallel to the drawing direction as compared to other semicrystalline polymers, such as nylon 6 and nylon 66, where the molecular orientation is prevented by the crystallites existing in original materials. Although in the case of PEN the crystallites are formed by strain-induced crystallization during drawing, a certain degree of strain-induced crystallization inhibits slippage among molecular chains and is effective in stretching amorphous chains, but an excessive crystallization prevents molecular chains from stretching. Therefore it is necessary to avoid (as much as possible) the crystallization during drawing and to fully orient amorphous chains in the drawing direction.

The optimum condition for the ZD treatment was determined by measuring birefringence (Δn) and degree of crystallinity (X_w) of the fibres drawn under various conditions: the condition giving higher Δn and lower X_w was chosen as optimum for the ZD treatment. To determine an optimum condition, the original PEN fibres were zone-drawn under various applied tensions (σ_a) at four different drawing temperatures (T_d).

Figure 2 shows Δn plotted as a function of σ_a at four different T_d values, ranging from 120 to 180°C. Δn increases monotonously up to 13 MPa with σ_a and thereafter the fibre at each T_d fails in a ductile manner when σ_a increases beyond 14 MPa. Δn value for fibre drawn at each T_d shows a maximum value under $\sigma_a = 13$ MPa; the fibre drawn at $T_d = 180$°C gives the highest Δn of 0.434. *Figure 3* shows the relations between draw ratios and Δn values for the fibres drawn at four different T_d values. Δn values of fibre drawn at each T_d increase almost linearly with increasing draw ratio. In general, Δn increases linearly with increasing draw ratio

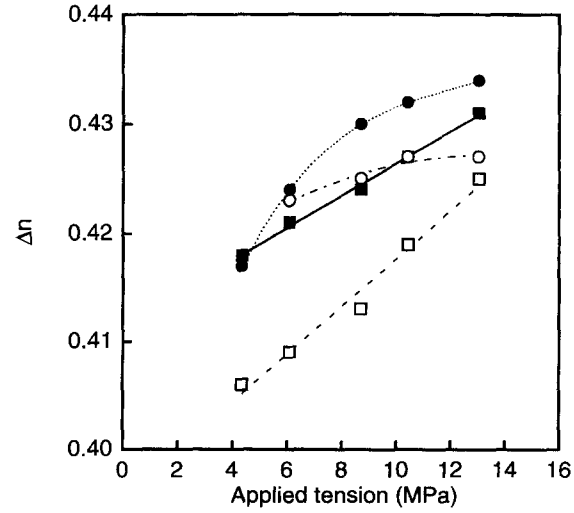

Figure 2 Changes in birefringence (Δn) of the zone-drawn fibres at four different drawing temperatures (T_d) with applied tension: (□) $T_d = 120$°C; (■) $T_d = 130$°C; (○) $T_d = 150$°C; (●) $T_d = 180$°C

at low draw ratios, but it levels off to reach a saturated value at higher ratios[38]. In the fibres zone-drawn in the temperature range of 120–180°C, however, such saturation is not observed; the linear relation is held even at higher draw ratios. The fact implies that the ZD treatments were effective in development of molecular orientation without the molecular relaxation. *Figure 4* shows the relations between X_w values and Δn values for the fibres drawn at four different T_d values. X_w values of the fibres drawn at T_d = 120 and 130°C are independent of increase in Δn and remain constant at about 30% and 32%, respectively. The trend at two lower T_d values shows that the evolution of orientation of amorphous regions has priority over the crystallization during the ZD treatment. Porter *et al.*[11] reported that PEN drawn below T_g crystallized less easily than that drawn above T_g.

On the other hand, X_w values of the fibres drawn at T_d = 150 and 180°C increase steadily with increasing Δn, and the fibre of T_d = 180°C has the maximum X_w of 38% at Δn = 0.434. It seems that not only the evolution of orientation of amorphous regions but also the crystallization occurs simultaneously in the drawings at T_d = 150 and 180°C. Consequently, the condition to produce the fibre with higher degree of orientation and lower degree of crystallinity, σ_a = 13 MPa and T_d = 130°C, was chosen as optimum for ZD treatment. The fibre drawn under the optimum condition is designated as the ZD fibre.

Determination of optimum condition for zone-annealing

The purpose of the ZA treatment is to crystallize the amorphous chains that were highly oriented by the ZD treatment without molecular relaxation. The optimum condition for the ZA treatment was also determined in the same way as in the case of the ZD treatment. *Figure 5* shows the changes in Δn of the fibres that were zone-annealed at four different annealing temperatures (T_a) with σ_a. At all T_a values, Δn increases steadily with increasing σ_a. The fibre annealed at T_a = 200°C under σ_a = 212 MPa gives the highest Δn of 0.473. *Figure 6* shows the relation between draw ratios and Δn values for the fibres zone-annealed under various conditions. In the ZA treatment at each T_a, Δn increases almost with increasing draw ratio. Although the fibre annealed at T_a = 210°C under σ_a = 182 MPa shows the maximum draw ratio of 8.5, its Δn is almost the same value as the fibre having a

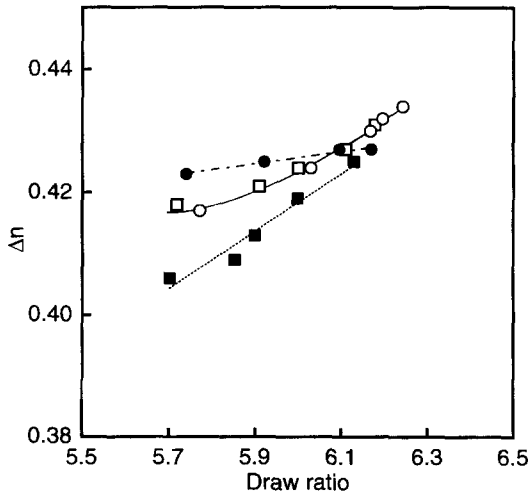

Figure 3 Relation between draw ratio and birefringence (Δn) for the zone-drawn fibres at four different drawing temperatures (T_d): (□) T_d = 120°C; (■) T_d = 130°C;○) T_d = 150°C;(●) T_d = 180°C

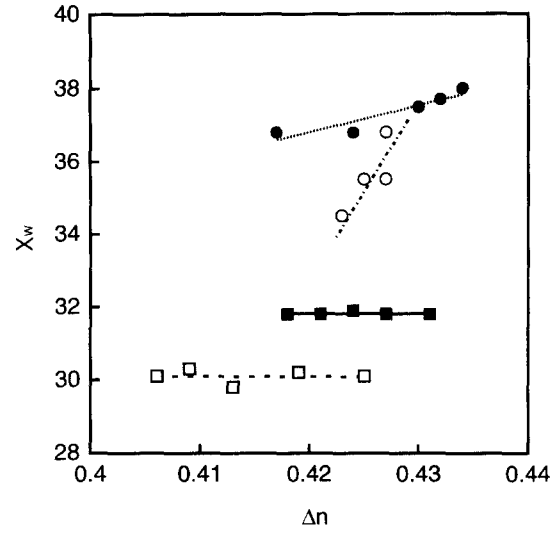

Figure 4 Relation between birefringence (Δn) and degree of crystallinity (X_w) for the zone-drawn fibres at four different drawing temperatures (T_d): (□) T_d = 120°C;(■) T_d = 130°C;(○) T_d = 150°C; (●) T_d = 180°C

draw ratio of 7.5, which was annealed at T_a = 160°C under σ_a = 212 MPa. The treatments at 210°C are less effective in development of molecular orientation as compared to the treatments at the lower T_d values.

Figure 7 shows the relation between X_w values and Δn values for the fibres annealed at four different T_a values. X_w increases with increasing Δn, increment in Δn is attributable to the additional crystallization and to the orientation of amorphous chains. Although X_w values of fibres annealed at T_a = 200 and 210°C are the same values (X_w = 40%), Δn of fibre annealed at T_a = 200°C under σ_a = 212 MPa is higher than that of the fibre annealed at T_a = 210°C under σ_a = 185 MPa. The difference in Δn suggests that the amorphous orientation of fibre annealed at T_a = 200°C is higher than that of the fibre annealed at T_a = 210°C.

Consequently, because the fibre annealed at T_a = 200°C under σ_a = 212 MPa has the highest Δn and the maximum X_w, this condition was chosen as optimum for the ZA treatment. Furthermore, though we attempted the second ZA treatment, tensile modulus could not be improved further by the second ZA treatment.

The optimum conditions for the ZD and ZA treatments are summarized in *Table 1*. The microstructure and mechanical properties of the fibre obtained under each optimum condition will be discussed below.

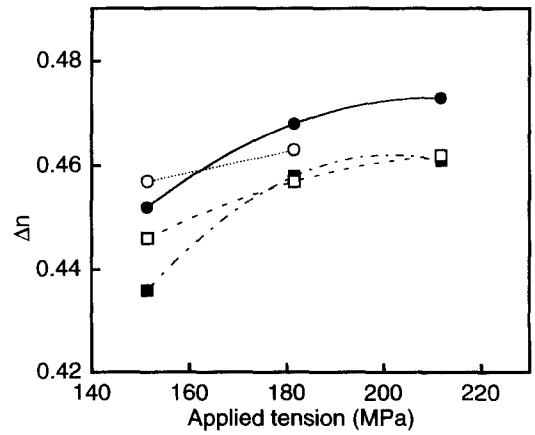

Figure 5 Changes in birefringence (Δn) of the zone-annealed fibres at four different annealing temperatures (T_a) with applied tension: (■) T_a = 160°C; (□) T_a = 180°C; (●) T_a = 200°C; (○) T_a = 210°C

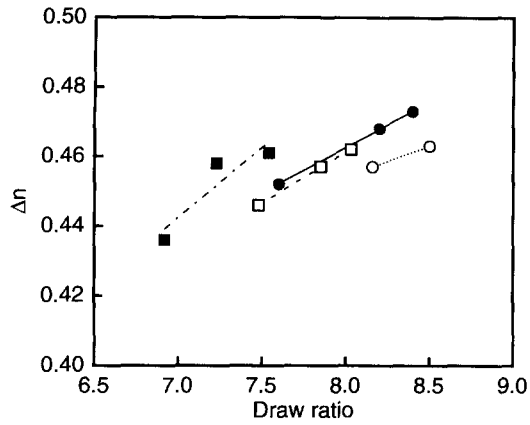

Figure 6 Relation between draw ratio and birefringence (Δn) for the zone-annealed fibres at four different annealing temperatures (T_a): (■) T_a = 160°C; (□) T_a = 180°C; (●) T_a = 200°C; (○) T_a = 210°C

Microstructure for the ZD and ZA fibres

Table 2 lists draw ratio (λ), Δn, X_w, and orientation factor of crystallites (f_c) for the original, ZD, and ZA fibres. Δn of the ZA fibre increases to 0.473 and is almost two times that of the ZA PET fibre [22]. The intrinsic Δn of PEN was reported to be 0.604, which was theoretically obtained by Aikawa[39]. X_w increases to 31% by the ZD treatment and further to 40% by the ZA treatment. The upper limit of usually observed X_w is about 50%[11], and the resulting X_w is 10% less than the upper limit value. The additional crystallization is presumably attributed to the increase in a number of crystallites and the crystal growth along the c axis during the treatments. Peszkin *et al.*[40] reported on the basis of WAXD and SAXS results that the additional crystallization in the oriented fibre took place along the fibre axis of the crystal already oriented. f_c increases up to 0.99 with only the ZD treatment and maintains a higher value even after subsequent ZA treatment. The development of crystallinity and orientation with processing can be qualitatively followed by the wide-angle X-ray diffraction photographs, as shown in *Figure 8*. The diffraction spots become more conspicuous with processing, and a sharpening of the diffraction spots indicates an improvement in crystal perfection. The three reflections (010, 100, and $\bar{1}10$) are observed in the equator and attributed to the α-form[41], but no (020) reflection due to the β-form is observed in the equator. It will be noted that the morphology of crystallites existing in the ZD and ZA fibres is only the α-form.

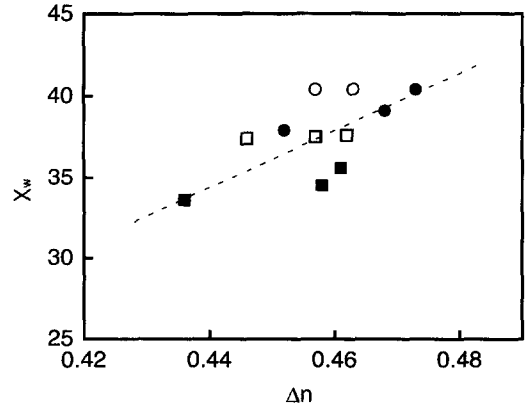

Figure 7 Relation between birefringence (Δn) and degree of crystallinity (X_w) for the zone-annealed fibres at four different annealing temperatures (T_a): (■) T_a = 160°C; (□) T_a = 180°C; (●) T_a = 200°C; (○) T_a = 210°C

Table 1 Optimum conditions for zone-drawing (ZD) and zone-annealing (ZA)

Treatment	Treating temperature (°C)	Applied tension (MPa)
ZD	130	13.0
ZA	200	212

Figure 9 shows a d.s.c. thermogram for each of the original, ZD, and ZA fibres. The d.s.c. thermogram of the original fibre shows a slight step due to change in the specific heat at about 125°C, which corresponds to the glass transition; an exothermic transition at 213°C caused by cold crystallization; and a melting endotherm peaking at 269°C. The ZD fibre has only a single sharp melting endotherm peaking at 271°C, and the ZA fibre has the endotherm peaking at 276°C. The increment in melting point is considered to be associated either with the change of crystal modification[42–44] or with an increase in crystal size and/or crystal perfection[45,46]. No change of the crystal modification occurs during the ZD and ZA treatments because only a single sharp melting peak is observed. Therefore, the melting point increase is attributed to an increase in the degree of perfection of the crystal. Buchner *et al.*[1] also suggested that no change of the crystal modification is observed during annealing of PEN.

Figure 10 shows the temperature dependence of thermal shrinkage for the original, ZD, and ZA fibres. The development of the thermal shrinkage during heating is associated with the chain coiling in the oriented amorphous regions[47] and is dependent on orientation of amorphous regions and the degree of crystallinity. The original fibre stretches rapidly above 140°C, and the stretch exceeds the instrumental limitation. The stretching behaviour of the original PEN fibre is the same as that of an original PPS fibre[31], but much different from that of the original PET fibre[48]. The PET fibre stretched rapidly in the temperature range of 70–100°C and gently above 100°C without the fluid-like deformation. The behaviour of the PET fibre suggested that the crystallites were formed by strain-induced crystallization in the temperature range of 70–100°C during the measurement, and then built up the physical network constraining the additional slippage of the chains. However, the rapid stretch of the original PEN fibre shows that strain-induced crystallization does not occur during the measurement, and that no network preventing the fluid-like deformation exists.

On the other hand, the ZD and the ZA fibres start to shrink slightly above 50°C as the temperature increases. The slight increase is attributable to a β-relaxation. The β-relaxation is associated with the motion of the naphthalene rings; the motions appear to involve rotations around the nearest oxygen–naphthyl links which are aligned along the main chain axis of the polymer[49]. The shrinkage for the ZD fibre increases slightly in the temperature range of 120–170°C, but decreases above about 170°C. The physical network in the ZD fibre was insufficient for constraint of the thermal shrinkage because of its low X_w, but the shrinkage with temperature decreases above 170°C because of an increase

Table 2 Draw ratio (λ), beirefringence (Δn), crystallinity (X_w), and crystallite orientation factor (f_c) for the original, ZD and ZA fibres

Fibre	λ	Δn	X_w (%)	f_c
Original	—	0.003	3.9	—
ZD	6.2	0.431	31	0.99
ZA	8.4	0.473	40	0.99

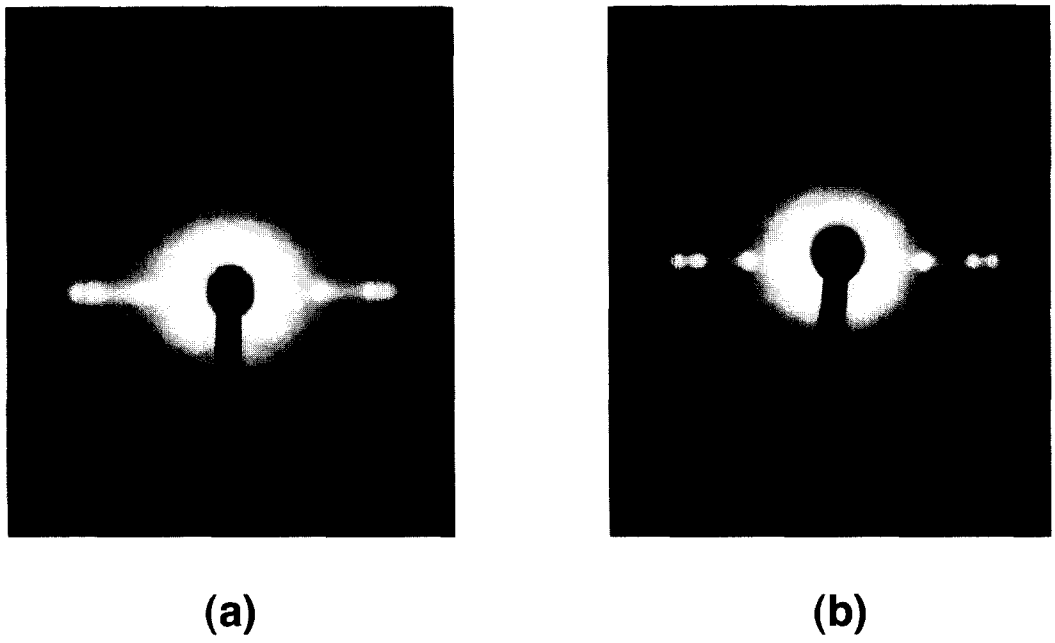

Figure 8 Wide-angle X-ray diffraction photographs of the ZD and ZA fibres: (a) ZD, (b) ZA

in the crosslink density resulting from additional crystallization during measurement[50]. In the case of the ZA fibres the slight increment of shrinkage in the temperature range of 120–170°C cannot be observed. The low in the ZA fibre is due to the higher crosslink density of the physical network which restricts the chain coiling.

Mechanical properties for the ZD and ZA fibres

Table 3 lists the tensile properties of the original, ZD, and ZA fibres. The tensile modulus and tensile strength increase with processing: the ZA fibre has a tensile modulus of 29 GPa and a tensile strength of 1.1 GPa. The tensile modulus of the ZA PEN fibre is higher than that of the ZA PET fibre[22] (about 20 GPa) and corresponds to about 20% of a theoretical value[14] (145 GPa at room temperature). The rate of attainment to the theoretical modulus is slightly higher than that (18%) of the ZA PET fibre[22].

Figure 11 shows the temperature dependence of the storage modulus (E'), for the original, ZD, and ZA fibres. E' values over a wide temperature range increase progressively with processing. E' for the original fibre decreases significantly at around 40°C and cannot be measured above the T_g because of fluid-like deformation caused by slippage among the amorphous chains. The significant decrease is attributed to the β-relaxation, which was not observed in the original PET[48] and PPS fibres[31]. E' values increase stepwise with the number of times in the treatment. Finally, E' of the ZA fibre reaches 30 GPa at 25°C. The pronounced decrease in E' due to the β-relaxation is also observed in the ZD and ZA fibres.

Figure 12 shows temperature dependence of tan δ for the original, ZD, and ZA fibres. The original fibre shows only the β-relaxation at 65°C. The ZD fibre shows the β-relaxation at about 70°C and an α-relaxation at about 165°C. The α-relaxation is considered to originate from the glass transition[49]. The β-relaxation of the ZD fibre decreases markedly in its peak height and broadens when compared with that of the original fibre. The ZA fibre gives the broad β-relaxation at 70°C and α-relaxation at 170°C, and the magnitude in the α-relaxation is about 1/2 that of the ZD fibre and is nearly the same as that in the β-relaxation. The α- and β-relaxation peaks shift to a higher temperature, decrease markedly in peak height, and become much broader with processing. The changes in position and in profile of the two peaks with processing indicates that the molecular mobility in the amorphous regions is restricted by the physical network with a higher degree of crosslink density.

CONCLUSION

The zone-drawing (ZD) and zone-annealing (ZA) method has been applied to PEN fibres to improve their mechanical properties. The optimum conditions for the ZD and ZA treatments were determined by measuring the birefringence (Δn) and degree of crystallinity (X_w).

To determine the ZD treatment condition, the ZD

Table 3 Tensile porperties of the original, ZD and Za fibres

Fibre	Tensile modulus (GPa)	Tensile strength (GPa)	Elongation at break (%)
Original	1.6	—	—
ZD	24	1.0	10.3
ZA	29	1.1	4.3

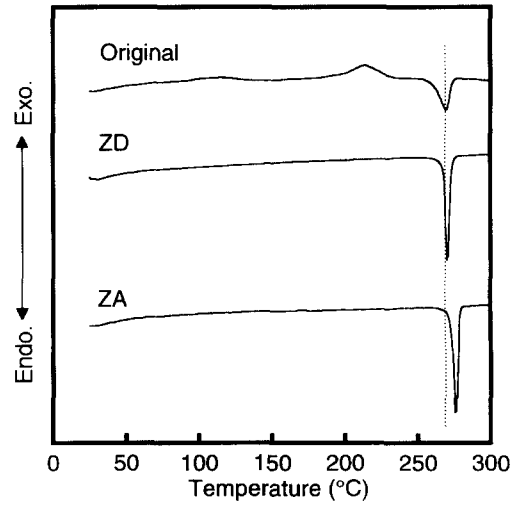

Figure 9 D.s.c. thermograms of the original, ZD, and ZA fibres

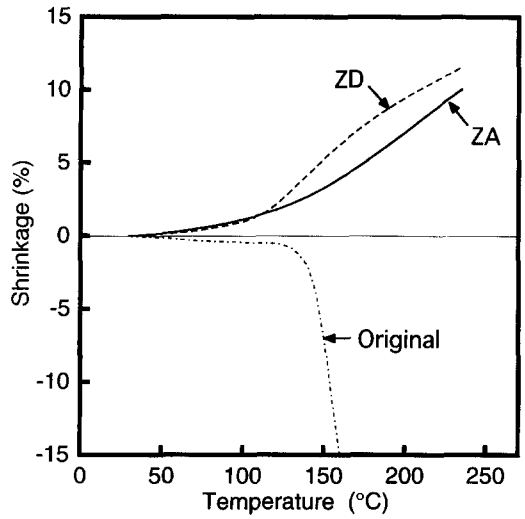

Figure 10 Temperature dependence of thermal shrinkage for the original, ZD, and ZA fibres

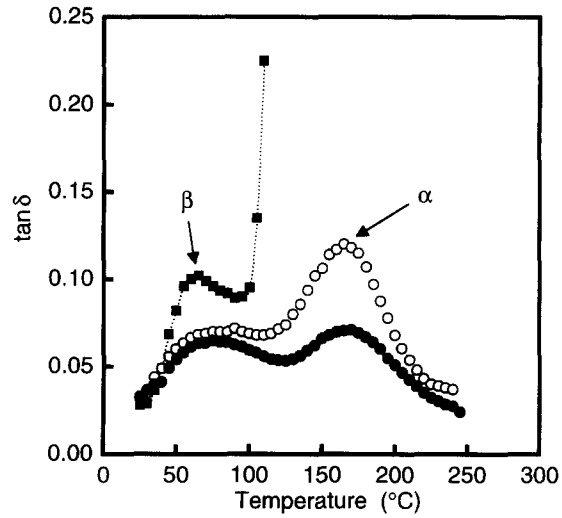

Figure 12 Temperature dependence of tan δ for the original, ZD, and ZA fibres: (■) original; (○) ZD; (●) ZA

treatments were carried out at various drawing temperatures (T_d) and applied tensions (σ_a). X_w values obtained were found to increase linearly with increasing Δn at $T_d = 150$ and 180°C, but to hold constant at $T_d = 120$ and 130°C (see *Figure 4*). This indicated that the strain-induced crystallization only proceeded at $T_d = 120$ and 130°C, and that not only the strain-induced crystallization but also the thermal crystallization, was induced at $T_d = 150$ and 180°C. Consequently, the ZD treatment at $T_d = 130$°C satisfied the purpose of the ZD treatment: its purpose is to avoid the thermal crystallization and to fully orient amorphous chains in the drawing direction.

To determine the optimum condition for the ZA treatment, the fibre zone-drawn under the optimum condition was zone-annealed at various annealing temperatures (T_a) and σ_a values. Δn and X_w values mostly increased with increasing T_a and σ_a, and the increment in Δn was attributed to the thermal crystallization. Although the fibres of $T_a = 200$ and 210°C had the highest X_w of 40%, Δn of the fibre of $T_a = 200$°C was higher than that of $T_a = 210$°C (see *Figure 7*). The difference in Δn between the two fibres indicated that molecular relaxation was induced in the ZA treatments at $T_a = 210$°C. Therefore the ZA treatment at $T_a = 200$°C was found to be optimum.

The ZD fibre obtained under the optimum condition had $X_w = 31\%$, $\Delta n = 0.431$, and orientation factor of crystallites of 0.99. The orientation factor increased remarkably up to 0.99 with only the ZD treatment. The ZA fibre obtained under the optimum condition had $X_w = 40\%$ and $\Delta n = 0.473$. Wide-angle X-ray diffraction photographs of the ZD and ZA fibres showed three reflections (010, 100, and $\bar{1}10$) attributed to the α-form crystal, but no (020) reflection attributed to the β-form was observed in the equator. Therefore, the crystallites existing in the ZD and ZA fibres are only the α-form crystal. The mechanical properties increased stepwise with processing, and the resulting ZA fibre showed a tensile modulus of 29 GPa and a tensile strength of 1.1 GPa.

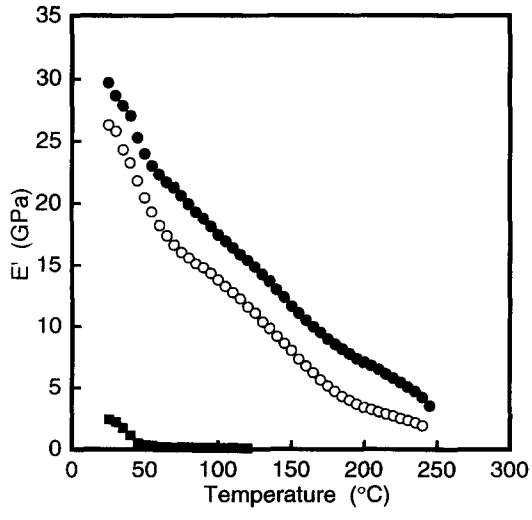

Figure 11 Temperature dependence of storage modulus (E') for the original, ZD and ZA fibres: (■) original; (○) ZD; (●) ZA

ACKNOWLEDGEMENTS

We are grateful to Teijin Ltd. for supplying PEN fibres to us.

REFERENCES

1. Buchner, S., Wiswe, D. and Zachmann, H.G., *Polymer*, 1989, **30**, 480.
2. Mencik, Z., *Chem Prum.*, 1967, **17**, 78.
3. Ülçer, Y. and Çakmak, M., *Polymer*, 1994, **35**, 5651.
4. Lu, X. and Windle, A.H., *Polymer*, 1995, **36**, 451.
5. Murakami, S., Nishikawa, Y., Tsuji, M., Kawaguchi, A., Kohjiya, S. and Cakmak, M., *Polymer*, 1995, **36**, 291.
6. Cakmak, M. and Lee, S.M., *Polymer*, 1995, **36**, 4039.
7. Abis, L., Merlo, E. and Pó, R., *J. Polym. Sci. Polym. Phys. Ed.*, 1995, **33**, 691.
8. Rueda, D.R., Varkalis, A., Viksne, A., Calleja, F.J.B. and Zachmann, H.G., *J. Polym. Sci. Polym. Phys. Ed.*, 1995, **33**, 1653.
9. Zhang, H., Rankin, A. and Ward, I.M., *Polymer*, 1996, **37**, 1079.
10. Jakeways, R., Klein, J.L. and Ward, I.M., *Polymer*, 1996, **37**, 3761.
11. Ghanem, A.M. and Porter, G.S., *J. Polym. Sci. Polym. Phys. Ed.*, 1989, **27**, 2587.
12. Ito, M., Honda, K. and Kanamoto, T., *J. Appl. Polym. Sci.*, 1992, **46**, 1013.
13. Nakamae, K., Nishino, T., Tada, K., Knamoto, T. and Ito, M., *Polymer*, 1993, **34**, 3322.
14. Nakamae, K., Nishino, T. and Gotoh, Y., *Polymer*, 1995, **36**, 1401.
15. Thistlethwaite, T., Jakeways, R. and Ward, I.M., *Polymer*, 1988, **29**, 61.
16. Acierno, D., La Mantia, F.P., Polizotti, G., Alfonso, G.C. and Ciferre, A.J., *Polym. Sci. Polym. Lett. Ed.*, 1977, **15**, 323.

17. Zachariades, A.E. and Poter, R.S., *J. Appl. Polym. Sci.*, 1979, **24**, 1371.
18. Richardson, A. and Ward, I.M., *J. Polym. Sci.*, 1981, **19**, 1549.
19. Gogolewski and Penneings, A.J., *Polymer*, 1985, **26**, 1394.
20. Fakirov, S. and Evstaiev, M., *Polymer*, 1990, **31**, 431.
21. Ito, M., Takahashi, K. and Kanamoto, T., *J. Appl. Polym. Sci.*, 1990, **40**, 1257.
22. Kunugi, T., Suzuki, A. and Hashimoto, M., *J. Appl. Polym. Sci.*, 1951, **1981**, 26.
23. Kunugi, T., *J. Polym. Sci. Polym. Lett.*, 1982, **20**, 329.
24. Kunugi, T., Ito, T. and Hashimoto, M., *J. Appl. Polym. Sci.*, 1951, **1983**, 28.
25. Kunugi, T., Akiyama, I. and Hashimoto, M., *Polymer*, 1982, **23**, 1199.
26. Kunugi, T., Suzuki, A. and Kubota, E., *Koubunshi Ronbunsyu*, 1992, **49**, 161.
27. Suzuki, A., Maruyama, S. and Kunugi, T., *Koubunshi Ronbunsyu*, 1992, **49**, 741.
28. Suzuki, A. and Endo, A., *Polymer*, 1997, **38**, 3085.
29. Kunugi, T., Kawasumi, T. and Ito, T., *J. Appl. Polym. Sci.*, 1990, **40**, 2101.
30. Kunugi, T., Suzuki, A. and Itoda, J., *Koubunshi Ronbunsyu*, 1990, **47**, 961.
31. Suziki, A., Kohno, T. and Kunugi, T., *J. Polym. Sci. Polym. Phys. Ed.* (in press).
32. Mencik, Z., *Chem. Prumysl*, 1967, **17**, 78.
33. Ouchi, I., Aoki, H., Shimotsuma, S., Asai, T. and Hosoi, M., in *Proceedings of the 17th Congress on Materials Resrarch.* Japan, 1974, p. 217.
34. Wilchinsky, Z.W., *J. Appl. Phys.*, 1963, **30**, 792.
35. Vittoria, V., De Candia, F., Capodanno, V. and Peterlin, A., *J. Polym. Sci. Polym. Phys. Ed.*, 1986, **24**, 1009.
36. Peterlin, A., *J. Polym. Sci.*, 1965, **69**, 61.
37. Wills, A.J., Capaccio, G. and Ward, I.M., *J. Polym. Sci. Polym. Phys. Ed.*, 1980, **18**, 493.
38. O'Neill, M.A., Duckett, R.A. and Ward, I.M., *Polymer*, 1988, **29**, 54.
39. Aikawa, Y., *Koubunshi Ronbunsyu*, 1994, **51**, 78.
40. Peszkin, P.N., Schultz, J.M. and Lin, J.S., *J. Polym. Sci. Polym. Phys. Ed.*, 1986, **24**, 2592.
41. Ülçer, Y. and Cakmak, M., *Polymer*, 1997, **38**, 2907.
42. Kalay, G., Zhong, Z., Allan, P. and Bevis, M.J., *Polymer*, 1996, **37**, 2077.
43. Yoshida, T., Fujiwara, Y. and Asano, T., *Polymer*, 1983, **24**, 925.
44. Tjong, S.C., Shen, J.S. and Li, R.K.Y., *Polymer*, 1996, **37**, 2309.
45. Mandelkern, L., Price, J.M., Gopalan, M. and Fatou, J.M.G., *J. Polym. Sci. A-2*, 1966, **4**, 385.
46. Taraiya, A.K., Unwin, A.P. and Ward, I.M., *J. Polym. Sci. Polym. Phys. Ed.*, 1988, **26**, 817.
47. Wilson, M.P.W., *Polymer*, 1974, **15**, 277.
48. Suziki, A., Sato, Y. and Kunugi, T., *J. Polym. Sci. Polym. Phys. Ed.* 1998, **36**, 473.
49. Blundell, D.J. and Buckingham, K.A., *Polymer*, 1985, **26**, 1623.
50. Perla, N.P. and Schultz, J.M., *J. Polym. Sci.*, 1986, **24**, 2591.